An algorithm of decomposition and combinatorial optimisation based on 3-Otsu

Liejun Wang*

School of Information Science and Engineering,
and
School of Software,
Xinjiang University,
Urumqi, 830046, China
Email: iejunaang@sina.com
*Corresponding author

Junhui Wu

School of Information Science and Engineering,
Xinjiang University,
Urumqi, 830046, China
Email: Junhui.W88@qq.com

Jiwei Qin

School of Education,
Shaanxi Normal University,
Xi'an, 710062, China
Email: uaibai@sina.com

Abstract: Recently, the 3-Otsu (three-dimensional maximum between-class variance algorithm) has drawn great attention in image segmentation. However the time consumption and calculation amount of 3-Otsu is large, so this paper provide a compositing 3-Otsu decomposed algorithm. Firstly, the histogram of 3-Otsu is resolved into three two-dimensional histogram by projecting and the projection plane is three coordinate plane of its own space. Secondly, the two-dimensional histogram formed after segmented by using 2-Otsu, then three segmentation results are obtained. Finally, three segmentation results are combined in linear manner and combination result is the output of segmentation result, under the ideal noise-free, Gaussian noise, salt noise, pepper noise and salt and pepper mixture noise, respectively. The results show that the proposed algorithm is nearly 30 times smaller in time consumption than 3-Otsu, although slightly more than 2-Otsu, its value is still small. Meanwhile the anti-noise performance, especially for mixed noise, is better than two other algorithms.

Keywords: three-dimensional Otsu; decomposition; reduction; linear combination.

Copyright © 2020 Inderscience Enterprises Ltd.

Reference to this paper should be made as follows: Wang, L., Wu, J. and Qin, J. (2020) 'An algorithm of decomposition and combinatorial optimisation based on 3-Otsu', *Int. J. Information and Communication Technology*, Vol. 16, No. 1, pp.68–83.

Biographical notes: Liejun Wang received his PhD degree in the School of Information and Communication Engineering from the Xi'an Jiaotong University in 2012. He is also a member of the Education Information Teach and Teaching Committee, member of the expert group for promoting domestic cryptography in key areas in the Xinjiang, Director of the Advisory Committee of Educational Information Technology Experts in the Xinjiang, Director of the main node of the China Education and Scientific Research Network in the Xinjiang and Deputy Director of the Network Centre. He has presided over four national projects related to network information security, two provincial and ministerial level, published more than 60 core papers. His current research interests include wireless sensor network, encryption algorithm and image intelligent processing.

Junhui Wu is now in the third year for his MS in Information and Engineering at the Xinjiang University. In 2017, He has participated in the research of Xinjiang Uygur face recognition method based on mobile internet. At the same time, He has also participated in the mentor's innovative team project. He current research interests are mainly image processing.

Jiwei Qin received her Master and PhD degrees in the School of Computer Architecture from the Xi'an Jiaotong University, Xi'an, China, in 2008 and 2013. She is currently an Engineer in the Network and Information Technology Center of the Xinjiang University. Her research interests include intelligent network, data mining, social network modelling and analysis, e-learning, recommender systems and collaborative filtering. She has directed and participated in quite a number of research projects and published papers in many international journals and conference proceedings, including Educational *Technology and Society*, *Sensors and Transducers*, *SAI Computing Conference*, etc.

1 Introduction

Image segmentation is not only an strong point which a beginner enter the image research gate, but also a key preprocessing step where computer vision, artificial intelligence and other fields go on conducting research the advanced image processing (Felzenszwalb and Huttenlocher, 2004; Garcia-Lamont et al., 2018).

In recent years, classification technology has been widely used in computer vision such as object detection, image retrieval (Wen and Wang, 2017) and target recognition and has achieved great success. Some useful attempts have been made in image segmentation. The method based on classification regards the image segmentation problem as the classification problem of a single pixel of the image. The labelled image is used as the training sample to train support vector machine, neural network (Cheng et al., 2018) and other classifiers and then the input image is classified by pixel by trained classifier. And image segmentation results are obtained according to pixel classification. However, this method makes the algorithm more complicated and consumes a lot of time.

Nowadays, there are some prevailing methods, such as segmentation based on graph theory, segmentation based on pixel clustering, semantic segmentation, threshold segmentation and so on (Jiang et al., 2017). Among them, the Otsu is heavily used in image segmentation because the principle is easy to understand and the idea is more concise (Nickfarjam et al., 2014). Otsu had been put forward in 1979 (Otsu, 1979), in order to solve the problem of weak anti-noise performance and enhance the ability of resisting external environment, Liu (1993) built 2-Otsu by introducing the neighbourhood mean, which solved the above problem, but it took more time and the operation complexity is higher; the algorithm was then expanded from one dimension to three dimensions by Jing et al. (2001) and Xiao et al. (2013) and the corresponding fast operation formula was given, there was no doubt that the anti-noise performance of the 3-Otsu is really strong, however, large computation and time consumption result in a consequence that it can't be applied in real time in practice. In this case, Fan et al. (2007) improved the defects in the literature Xiao et al. (2013) and gave an accurate and fast iterative algorithm. Wang et al. (2012) changed the structure of three-dimensional histogram, rejected the search way of enumeration and introduced new division regional mode and fast recursive formula; Lei et al. (2008) also gave a quick way of arithmetic and inferred the relevant content; Zhiwei et al. (2016) optimised the optimisation process of 3-otsu by using the FA combined with Les flight, to reduce the time consumption. These similar methods have their advantages and disadvantages, but none of them can solve the problem better. And Shen et al. (2011) reestablished the histogram which is reduced from three dimension to one dimension by studying the distribution of noise points. Under the fast recursion and look up table or other methods, not meeting the requirements for practical application of engineering; Liu et al. (2014) provided a new viewpoint for solving the problem, which increased speed and reduced operation by the three-dimensional histogram grouping rebuilt; Qing and Fang (2017) has realised the reduction of the 3-Otsu dimensionality and cut down the time consumption of the algorithm by using the projection decomposition technique; Zhang et al. (2016) has applied 3-Otsu decomposition into the segmentation of bone tissue and obtained better results; Lin et al. (2013) has adopted the weighted method to solve the problem of poor segmentation effect when the noise is strong; Liu et al. (2018) has solved the problem of low efficiency and low accuracy of image segmentation model by the means of weighted fitting energy.

In view of this, this paper proposes a kind means of combination optimisation which is on the basis of 3-Otsu decomposition. The three-dimensional histogram is mapped to three mutually perpendicular two-dimensional plane through the projection technology and the 3-Otsu is transformed into 2-Otsu.Then the 2-Otsu segmentation was implemented and the segmentation results which are combined by linear combination as output. The experimental results show that the proposed algorithm has better anti-noise performance and less time consumption, which can effectively deal with the above problems. So our main contributions are summarised as followings:

1 We propose a kind means of combination optimisation which is on the basis of 3-pysu decomposition.

2 The three-dimensional histogram is mapped to three mutually perpendicular two-dimensional plane through the projection technology and the 3-otsu is transformed into 2-Otsu.

3 The 2-Otsu segmentation was implemented and the segmentation results which are combined by linear combination as output.

2 The main work

2.1 3-Otsu image segmentation algorithm

2.1.1 Two definitions

1 Definition of neighbourhood mean

The neighbourhood mean of the image is obtained through an $N \times N$ template wandering in the image, N is an integer. The coefficients in the template are generally set to 1 and the problem of weighted average is not considered here. Then, the neighbourhood mean $g(m, n)$ is defined as follows:

$$g(m,n) = \frac{1}{N \times N} \sum_{i=-(N-1)/2}^{(N-1)/2} \sum_{j=-(N-1)/2}^{(N-1)/2} f(m+i, n+j) \tag{1}$$

2 Definition of neighbourhood values

The template and coefficient are selected in the neighbourhood value which is the same as the neighbourhood mean. The neighbourhood values $h(m, n)$ are defined as follows:

$$h(m,n) = Med\left\{ \sum_{i=-(N-1)/2}^{(N-1)/2} \sum_{j=-(N-1)/2}^{(N-1)/2} f(m+i, n+j) \right\} \tag{2}$$

2.1.2 3-Otsu image segmentation algorithm

The size of the image is $M \times N$, for the sake of building a three-dimensional rectangular coordinate system, the gray value is used as the horizontal axis, the neighbourhood mean is used as the vertical axis and the neighbourhood values are used as vertical shaft. Suppose the greyscale value of all pixels in the image is $f(m, n)$,$0 \le f(m, n) \le -1$. Then the neighbourhood mean $g(m, n)$, which is given in Section 2.1.1, $0 \le g(m, n) \le L - 1$. In the same way, for the neighbourhood value $h(m, n)$, $0 \le h(m, n) \le L - 1$.

The three-dimensional histogram is constructed by $f(m, n)$, $g(m, n)$, $h(m, n)$, which is shown in Figure 1(a). We say that the value at (i, j, k) is P_{ijk} and the number of times that $f(m, n) = i$, $g(m, n) = j$, $h(m, n) = k$ appears at the same time is C_{ijk}. The P_{ijk} is the proportion of C_{ijk} in the total, so

$$P_{ijk} = \frac{C_{ijk}}{M \times N} \tag{3}$$

where $0 \le i, j, k \le L - 1$ and $\sum_{i=0}^{L-1} \sum_{j=0}^{L-1} \sum_{k=0}^{L-1} P_{ijk} = 1$

Figure 1 Three-dimensional histogram, (a) three-dimensional histogram constructed (b) division of blocks in each region (c) the lower four pieces 0, 2, 3, 4 (d) the top four pieces 4, 5, 6, 1, 7

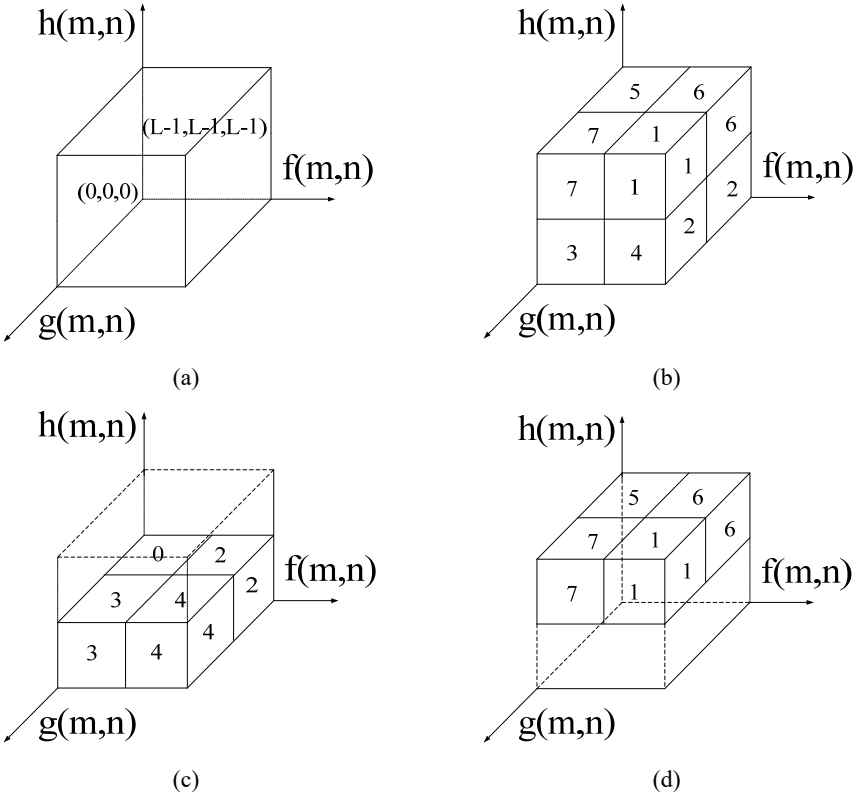

In the cube space region which the side length is L-1, the three dimensional histogram is divided into eight modules by any three-dimensional coordinate point, as it is shown in Figure 1(b). And then, the lower four modules are shown in Figure 1(c) and the upper four modules are shown in Figure 1(d). In Liu (1993), the value of P_{ijk} is about 0 in the module 2–7, so we assume that the modules 0 and 1 represent the target X_0 and the background X_1 respectively (both of which are equal and vice versa). Therefore:

$$\sum\nolimits_{a\subset A} P_{ijk} \approx 0,\ 0 \le i,\ j,\ k \le L-1, \quad A = 2, 3, 4, 5, 6\ 7. \tag{4}$$

$$\sum\nolimits_{b\subset B} P_{ijk} \approx 1,\ 0 \le i,\ j,\ k \le L-1, \quad B = 0, 1. \tag{5}$$

For any (s, t, q), ω_0 and ω_1, is the probability of μ_0 and μ_1 appear in module 0 and 1, should be:

$$\omega_0 = \sum_{i=0}^{s}\sum_{j=0}^{t}\sum_{k=0}^{q} P_{ijk} = \omega_0(s, t, q) \tag{6}$$

$$\omega_1 = \sum_{i=s+1}^{L-1}\sum_{j=t+1}^{L-1}\sum_{k=q+1}^{L-1} P_{ijk} = \omega_1(s,t,q) \tag{7}$$

X_0 and X_1 in module 0 and 1 respectively mean μ_0 and μ_1 coordinates:

$$\begin{aligned}\mu_0 &= \left(\mu_{0i}, \mu_{0j}, \mu_{0k}\right)^T \\ &= \left(\sum_{i=0}^{s}\sum_{j=0}^{t}\sum_{k=0}^{q}\frac{iP_{ijk}}{\omega_0(s,t,q)}, \sum_{i=0}^{s}\sum_{j=0}^{t}\sum_{k=0}^{q}\frac{jP_{ijk}}{\omega_0(s,t,q)}, \sum_{i=0}^{s}\sum_{j=0}^{t}\sum_{k=0}^{q}\frac{kP_{ijk}}{\omega_0(s,t,q)}\right)^T\end{aligned} \tag{8}$$

$$\begin{aligned}\mu_1 &= \left(\mu_{1i}, \mu_{1j}, \mu_{1k}\right)^T \\ &= \left(\sum_{i=s+1}^{L-1}\sum_{j=t+1}^{L-1}\sum_{k=q+1}^{L-1}\frac{iP_{ijk}}{\omega_1(s,t,q)}, \sum_{i=s+1}^{L-1}\sum_{j=t+1}^{L-1}\sum_{k=q+1}^{L-1}\frac{jP_{ijk}}{\omega_1(s,t,q)}, \sum_{i=s+1}^{L-1}\sum_{j=t+1}^{L-1}\sum_{k=q+1}^{L-1}\frac{kP_{ijk}}{\omega_1(s,t,q)}\right)^T\end{aligned} \tag{9}$$

The total average coordinates μ_T of all points in a three-dimensional histogram is:

$$\begin{aligned}\mu_T &= \left(\mu_{Ti}, \mu_{Tj}, \mu_{Tk}\right)^T \\ &= \left(\sum_{i=0}^{L-1}\sum_{j=0}^{L-1}\sum_{k=0}^{L-1} iP_{ijk}, \sum_{i=0}^{L-1}\sum_{j=0}^{L-1}\sum_{k=0}^{L-1} jP_{ijk}, \sum_{i=0}^{L-1}\sum_{j=0}^{L-1}\sum_{k=0}^{L-1} kP_{ijk}\right)^T\end{aligned} \tag{10}$$

We view the whole three-dimensional histogram as the complete U and from the above, we know that U is equal to A plus B:

$$\begin{aligned}\sum_{U} P_{ijk} &= \sum_{A} P_{ijk} + \sum_{B} P_{ijk} \\ \sum_{i=0}^{L-1}\sum_{j=0}^{L-1}\sum_{k=0}^{L-1} P_{ijk} &= \sum_{i=0}^{L-1}\sum_{j=0}^{L-1}\sum_{k=0}^{L-1} P_{ijk} + \sum_{i=0}^{L-1}\sum_{j=0}^{L-1}\sum_{k=0}^{L-1} P_{ijk} + 0 \\ &= \omega_0 + \omega_1 \\ &= \omega_0(s,t,q) + \omega_1(s,t,q)\end{aligned} \tag{11}$$

where A, B and U are the same as the previous ones.

The discrete measure matrix H of class X_0 and X_1 is given as follows:

$$\begin{aligned}H &= \omega_0\left[\left(\mu_0 - \mu_T\right)\left(\mu_0 - \mu_T\right)^T\right] + \omega_1\left[\left(\mu_1 - \mu_T\right)\left(\mu_1 - \mu_T\right)^T\right] \\ &= \begin{bmatrix} a_{00} & a_{01} & a_{02} \\ a_{10} & a_{11} & a_{12} \\ a_{20} & a_{21} & a_{22} \end{bmatrix}\end{aligned} \tag{12}$$

3-Otsu uses the trace of matrix H as the distance measure function and the trace of H is the sum of the three elements a_{00}, a_{11} and a_{22} on the main diagonal line.

And

$$\begin{aligned} a_{00} &= \omega_0 \left(\mu_{0i} - \mu_{Ti}\right)^2 + \omega_1 \left(\mu_{1i} - \mu_{Ti}\right)^2 \\ a_{11} &= \omega_0 \left(\mu_{0j} - \mu_{Tj}\right)^2 + \omega_1 \left(\mu_{1j} - \mu_{Tj}\right)^2 \\ a_{22} &= \omega_0 \left(\mu_{0k} - \mu_{Tk}\right)^2 + \omega_1 \left(\mu_{1k} - \mu_{Tk}\right)^2 \end{aligned} \tag{13}$$

So

$$\begin{aligned} t_r(H(s,t,q)) &= a_{00} + a_{11} + a_{22} \\ &= \omega_0 \left(\mu_{0i} - \mu_{Ti}\right)^2 + \omega_1 \left(\mu_{1i} - \mu_{Ti}\right)^2 \\ &+\omega_0 \left(\mu_{0j} - \mu_{Tj}\right)^2 + \omega_1 \left(\mu_{1j} - \mu_{Tj}\right)^2 \\ &+\omega_0 \left(\mu_{0k} - \mu_{Tk}\right)^2 + \omega_1 \left(\mu_{1k} - \mu_{Tk}\right)^2 \\ &= \omega_0 \left[\left(\mu_{0i} - \mu_{Ti}\right)^2 + \left(\mu_{0j} - \mu_{Tj}\right)^2 + \left(\mu_{0k} - \mu_{Tk}\right)^2 \right] \\ &+\omega_1 \left[\left(\mu_{1i} - \mu_{Ti}\right)^2 + \left(\mu_{1j} - \mu_{Tj}\right)^2 + \left(\mu_{1k} - \mu_{Tk}\right)^2 \right] \\ &= \frac{\left[\omega_0(s,t,q)\mu_{Ti} - \mu_i(s,t,q)\right]^2}{\omega_0(s,t,q)(1-\omega_0(s,t,q))} + \frac{\left[\omega_0(s,t,q)\mu_{Tj} - \mu_j(s,t,q)\right]^2}{\omega_0(s,t,q)(1-\omega_0(s,t,q))} \\ &+ \frac{\left[\omega_0(s,t,q)\mu_{Tk} - \mu_k(s,t,q)\right]^2}{\omega_0(s,t,q)(1-\omega_0(s,t,q))} \end{aligned} \tag{14}$$

where $\omega_0(s, t, 1)$, μ_{Ti}, μ_{Tj}, μ_{Tk} are the same as the previous ones and $\mu_i(s, t, q)$, $\mu_j(s, t, q)$, $\mu_j(s, t, q)$ is given as follows:

$$\begin{aligned} \mu_i(s,t,q) &= \sum_{i=0}^{s}\sum_{j=0}^{t}\sum_{k=0}^{q} iP_{ijk} \\ \mu_j(s,t,q) &= \sum_{i=0}^{s}\sum_{j=0}^{t}\sum_{k=0}^{q} jP_{ijk} \\ \mu_k(s,t,q) &= \sum_{i=0}^{s}\sum_{j=0}^{t}\sum_{k=0}^{q} kP_{ijk} \end{aligned} \tag{15}$$

The coordinate vector B when A is the largest is the optimal threshold vector value. The advantage of the 3-otsu algorithm is higher resistance to noise, stronger adaptability to external situation and powerful generalisation. However, all of these are obtained by making complicated operations and consuming a large amount of time. The real time in practical application cannot be achieved, which is the crux of the problem.

2.2 The flow chart

The flow chart of the decomposition combinatorial optimisation algorithm based on 3-Otsu is shown in Figure 2. The basic knowledge of 3-Otsu has been introduced in Section 2.1. The 3-Otsu decomposed into three 2-Otsu by projection and then the image segmentation is introduced in Section 2.3.1. The combined optimisation of segmentation results will be in Section 2.3.2.

Figure 2 Flow chart of the algorithm

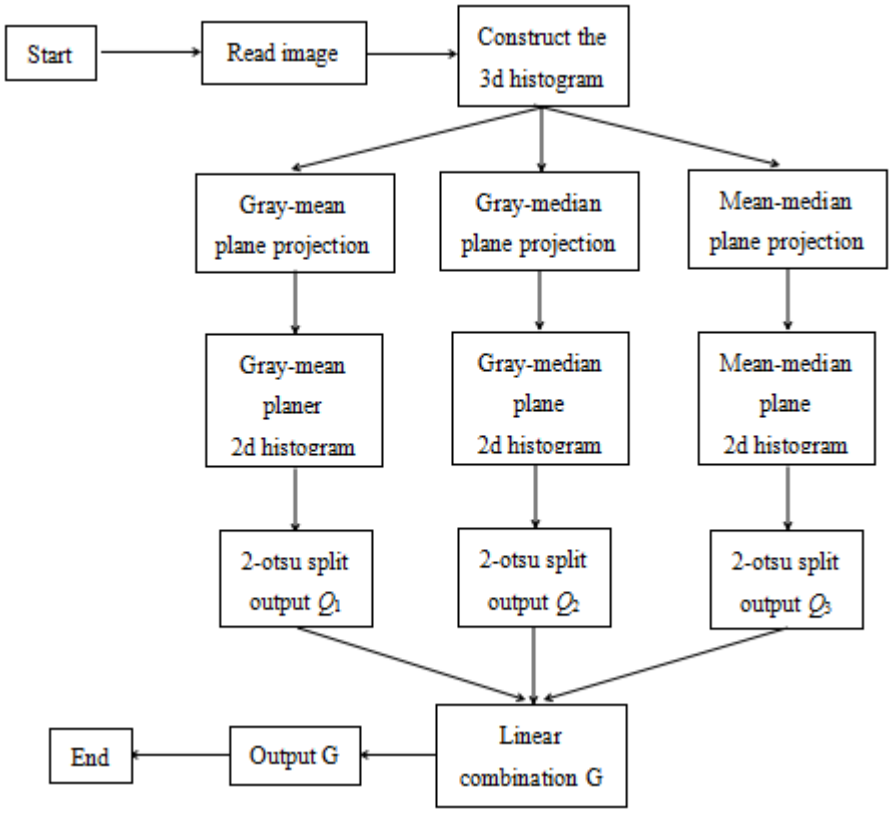

2.3 3-Otsu decomposition and combinatorial optimisation algorithm

2.3.1 Decomposition 3-Otsu

If the range of the image greyscale is [0, L – 1], according to the definition mentioned above, a three-dimensional histogram which the side length of the cube space region is L-1 will be formed in a three-dimensional coordinate system constructed in a gray value – neighbourhood mean – neighbourhood value, as shown in Figure 3(a). Firstly, the three-dimensional histogram is projected to the gray value-neighbourhood mean plane, gray value – neighbourhood value plane, neighbourhood mean – neighbourhood value plane. Three two-dimensional histogram can be obtained respectively from the three-dimensional histogram in the three vertical two-dimensional coordinate planes as shown in Figures 3(b) to 3(d). The purpose of converting a three-dimensional histogram to a two-dimensional histogram is achieved. The 2-Otsu algorithm is used to perform image segmentation in two-dimensional histogram which is derived from the projection of the three two-dimensional planes. We use projection to transform a three-dimensional into three two-dimensional to achieve dimensionality reduction.

Figure 3 Three-dimensional histogram projections, (a) three-dimensional histogram of the space coordinate system (b) two-dimensional histogram of gray – mean plane (c) two dimensional histogram of gray – median plan (d) two-dimensional histogram of mean – median plane

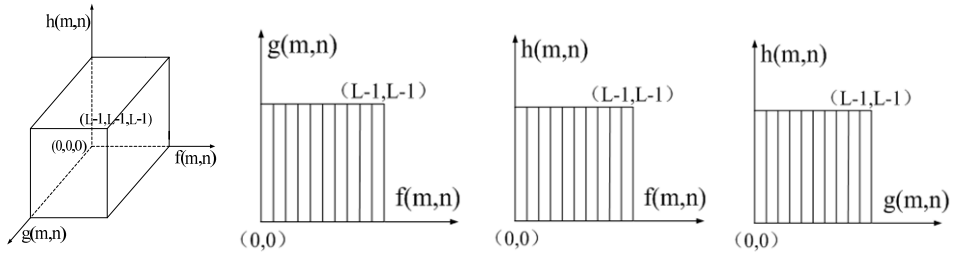

(a) (b) (c) (d)

2.3.2 Combinatorial optimisation segmentation results

Assuming that the above three 2-Otsu image segmentation results are Q_1, Q_2 and Q_3, the linear weighted combination is performed according to the following formula:

$$G = k_1 Q_1 + k_2 Q_2 + k_3 Q_3 \tag{16}$$

where G is output of the final segmentation result, k_1, k_2, k_3 is the adjustment coefficient of the linear weighted combination, whose value is closely related to the final output result and the appropriate value should be selected according to different situations.

The pseudo-code of the algorithm is as follows:

1 Read in the image to be segmented.

2 Set the value of k1, k2 and k3.

3 Construct the three-dimensional histogram of the image according to the 3-Otsu algorithm.

4 The three-dimensional histogram is projected to three coordinate planes respectively and three two-dimensional histograms are obtained from the projection results

5 2-Otsu image segmentation algorithm was performed on three two-dimensional histogram respectively and the output results are Q1, Q2 and Q3

6 According to (16), the linear combination of Q1, Q2 and Q3 is conducted and the output result G is the segmentation result.

3 Experimental results and analysis

3.1 Experimental results and analysis

In this paper, our experiments are implemented using MATLAB(R2016b) on a PC with an Intel® Core™ i3-2130 CPU @ 3.40GHZ , 4.0GB RAM. It mainly includes the

following contents: after investigation, it is generally accepted that Lena diagram, Camera diagram and Rice plot were used to test the performance of the proposed algorithm under the conditions of non-noise, Gaussian noise, salt noise and pepper noise, Gaussian noise and salt and pepper noise respectively. When there is noise, the noise intensity will be set to 0.001. On the basis of the above conditions, the segmentation results of fast 2-Otsu, 3-Otsu and the proposed algorithm are used to make comparisons mutually as shown in Figures 4~7. The direct observation of segmentation results can be concluded as follows:

1 When the non-noise segmentation results are observed in Figure 4, the segmentation results of Lena diagram are as follows: compared with fast 2-Otsu and 3-Otsu, the proposed algorithm is more clear at the top edge of hat and more details are kept on the left side of brim. There are more traces of eyelashes and left sideburns and so on. As you can see in the segmentation results of the Camera diagram, fast 2-otsu facial expression is preserved greatly, the best overall effect is 3-Otsu, and advantages of the proposed algorithm are relatively clean in the background. The following conclusions can be obtained from the segmentation results of Rice graph. Fast 2-Otsu has the worst segmentation effect. There are some obscure grains of rice at the bottom and more interference points on the top. The proposed algorithm is better than 3-Otsu. There are more grains of rice in the lower part, but at the top there are also several interference points left.

2 When the segmentation results of Gaussian noise are showed in Figure 5. Contrasting the three segmentation results, fast 2-Otsu has the much noise points left, the noise points of the proposed algorithm in Lena diagram are filtered out the most. 3-Otsu has a few scattered noise points to be retained. The noise points in the Camera diagram are mainly concentrated in the background and the proposed algorithm is not much different from the 3-Otsu effect. In Rice diagram, the proposed algorithm only has some Rice grain shape in the lower part than the 3-Otsu.

3 When the segmentation result of adding the salt and pepper noise is analysed in Figure 6. For fast 2-Otsu, the upper part in the Lena hat and the man's body in the Camera photograph have obvious noise retention, The overall denoising effect of Rice diagram is not good. The proposed algorithm is good, except for a flaw in the frame of the camera in the Camera photograph. 3-Otsu has a good segmentation of Lena diagram, but there are obvious noise points on the body of the Camera photograph. There are noise points in the Rice diagram and the lower part is a little bad.

4 When the segmentation result of the mixed noise of Gaussian and pretzel is discussed in Figure 7, it is obvious that the proposed algorithm segmentation effect is better. Fast 2-Otsu and 3-Otsu have some problems and there are obvious noise points which are not filtered out in the segmentation results.

Figure 4 No noise segmentation results, (a) original image (b) rapid 2-Otsu segmentation results (c) 3-Otsu segmentation results (d) segmentation results of the proposed algorithm

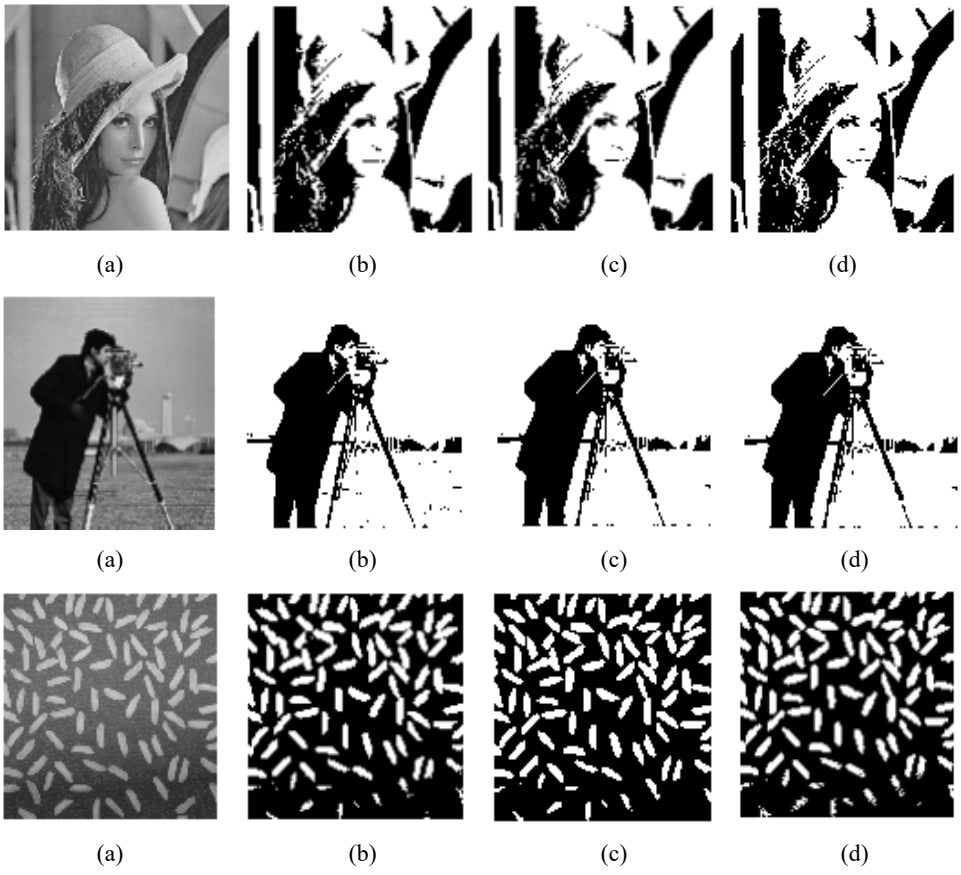

Figure 5 Segmentation result of adding Gaussian noise, (a) source image plus Gaussian noise (b) rapid 2-otsu segmentation results (c) 3-Otsu segmentation results. (d) segmentation results of the proposed algorithm

Figure 5 Segmentation result of adding Gaussian noise, (a) source image plus Gaussian noise (b) rapid 2-otsu segmentation results (c) 3-Otsu segmentation results. (d) segmentation results of the proposed algorithm (continued)

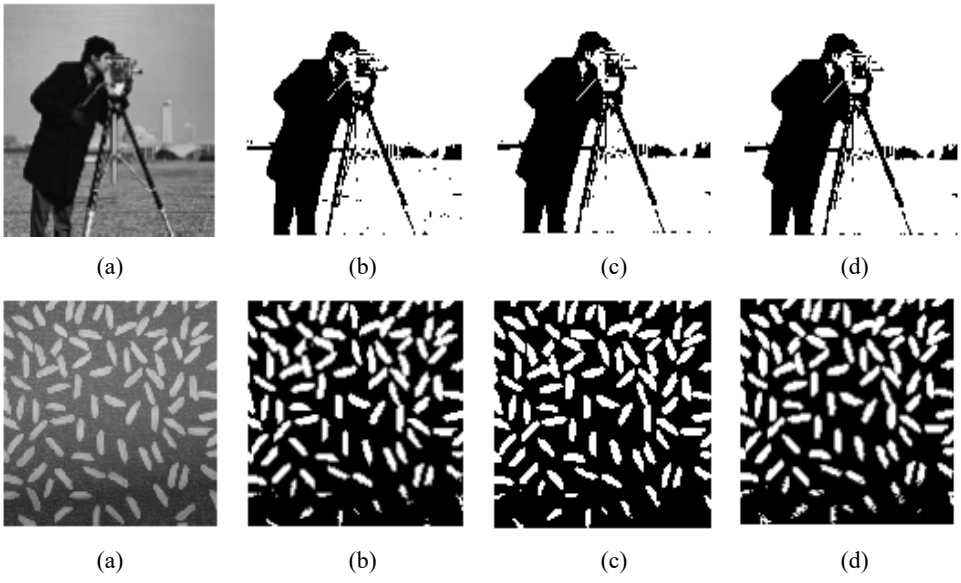

(a) (b) (c) (d)

(a) (b) (c) (d)

Figure 6 Segmentation result of adding salt and pepper noise, (a) source image with salt and pepper noise (b) rapid 2-Otsu segmentation results (c) 3-Otsu segmentation results (d) segmentation results of the proposed algorithm

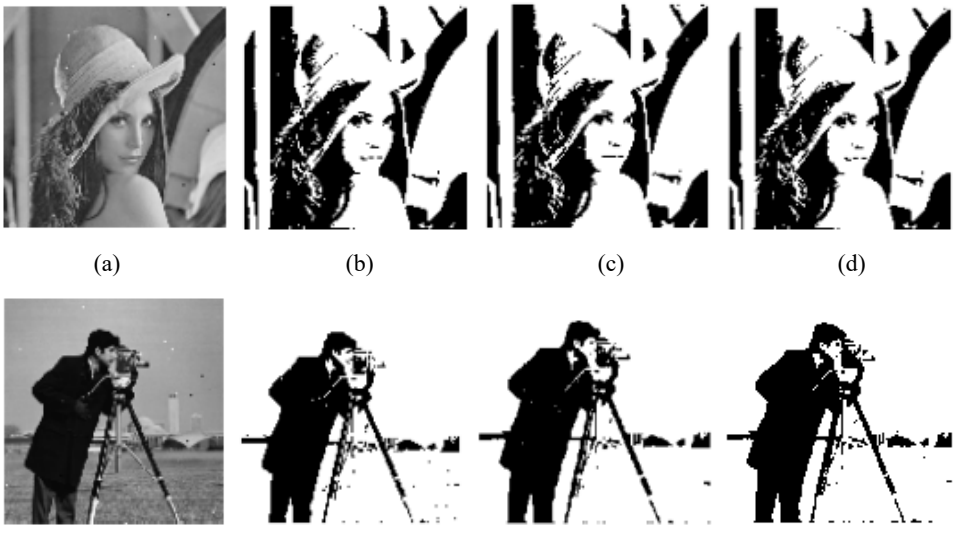

(a) (b) (c) (d)

(a) (b) (c) (d)

Figure 6 Segmentation result of adding salt and pepper noise, (a) source image with salt and pepper noise (b) rapid 2-Otsu segmentation results (c) 3-Otsu segmentation results (d) segmentation results of the proposed algorithm (continued)

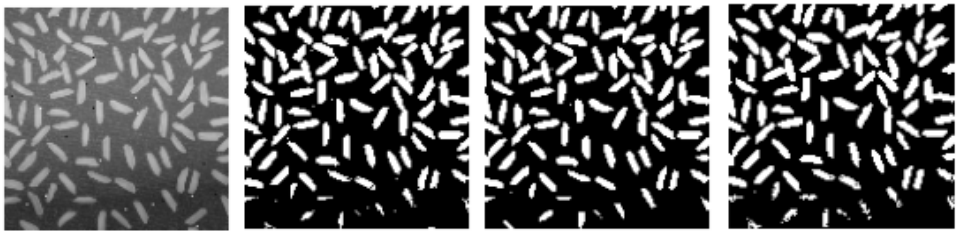

(a) (b) (c) (d)

Figure 7 Segmentation result of mixing Gaussian and pretzel noise, (a) source image with Gaussian and pretzel noise (b) rapid 2-Otsu segmentation results (c) 3-Otsu segmentation results (d) segmentation results of the proposed algorithm

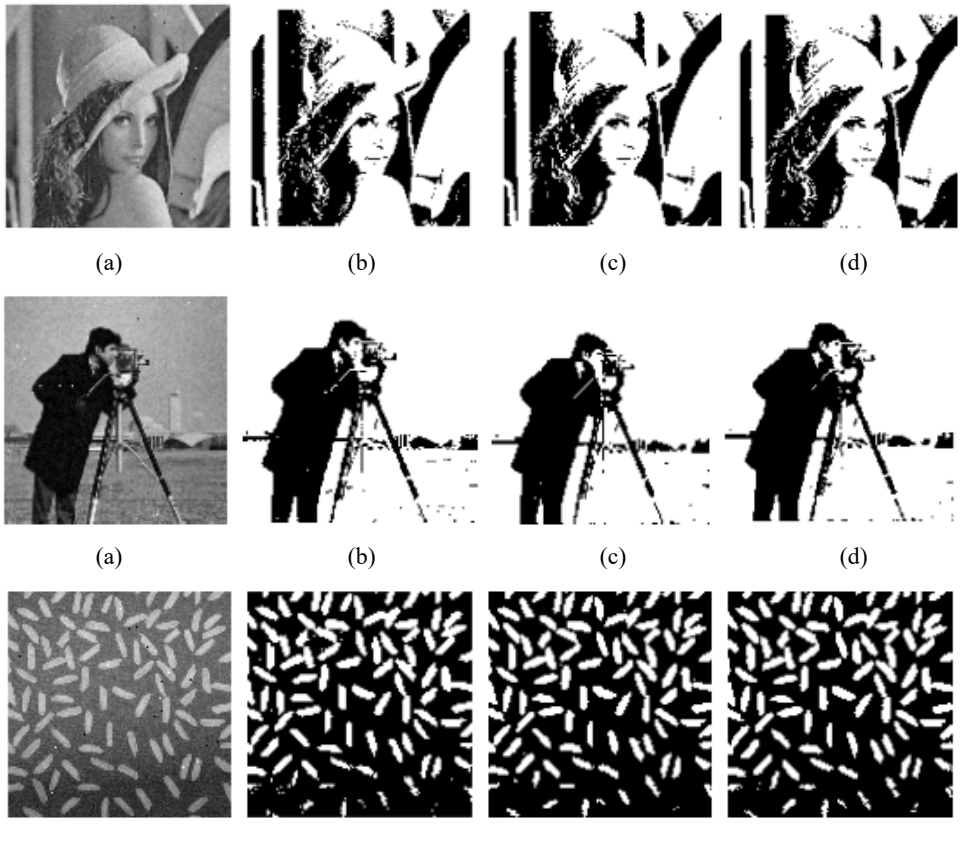

(a) (b) (c) (d)

(a) (b) (c) (d)

(a) (b) (c) (d)

3.2 The algorithm running time

The performance of proposed algorithm can not only see its segmentation effect, but also must consider the running time. When the running time is too much, even if the effect is better, there is no practical application value. Under the same hardware and software and almost invariable surroundings, the running time of the proposed algorithm is not constant every time, but fluctuations in a small range. Therefore, in this paper, the algorithm is executed 20 times and the average value of 20 times is regarded as the standard of evaluation time. In the four cases mentioned above, the average time of the execution of the algorithm is shown in Tables 1 to 4. It is apparent that the time of fast 2-Otsu is the shortest and the fastest. However, it is known that the anti-noise performance is the weakest and the segmentation effect is poor. Although the proposed algorithm is not as fast as fast 2-Otsu, the average difference between the proposed algorithm and fast 2-Otsu is less than one second. 3-Otsu has the largest time and the slowest speed. The proposed algorithm is more than 30 times higher than that of 3-Otsu. In conclusion, considering the factors such as noise resistance, segmentation time and segmentation effect, the proposed algorithm is a better algorithm.

Table 1 algorithm running time without noise (unit\second)

	Lena	*Camera*	*Rice*
Fast 2-Otsu	0.23546015	0.23240415	0.22067265
3-Otsu	31.8196318	32.6091274	31.65370325
Proposed algorithm	1.0172401	0.822314	0.8169673

Table 2 algorithm running time with Gaussian noise (unit\second)

	Lena	*Camera*	*Rice*
Fast 2-Otsu	0.24696735	0.23642845	0.22928155
3-Otsu	32.00749005	32.1805765	31.6420133
Proposed algorithm	1.0194646	0.8604513	0.8478941

Table 3 algorithm running time with salt and pepper noise (unit\second)

	Lena	*Camera*	*Rice*
Fast 2-Otsu	0.24394205	0.24139515	0.22825035
3-Otsu	32.1626214	31.9406496	31.68622975
Proposed algorithm	1.02409965	0.86311175	0.82998935

Table 4 algorithm running time with mixing Gaussian and salt and pepper noise (unit\second)

	Lena	*Camera*	*Rice*
Fast 2-Otsu	0.24965345	0.23831735	0.2398468
3-Otsu	32.29019775	32.69716085	31.94577155
Proposed algorithm	1.07936035	0.86615325	0.86401195

4 Conclusions

This paper puts forward a combinatorial optimisation method based on 3-Otsu decomposition. In this algorithm, it is not necessary to obtain the optimal threshold from 3-Otsu. Instead, the 3-Otsu is transformed into three 2-Otsu by projection and then the 2-Otsu image segmentation is performed. The segmentation consequences are combined in a linear manner, the output of the combination is the final conclusion. The results show that the time difference is small, compared with 2-Otsu, the proposed algorithm has stronger anti-noise performance and higher segmentation quality, on the basis of slightly stronger anti-noise performance, contrasted with 3-Otsu, the time consumption of the proposed algorithm has been reduced by more than 30 times and it provides a new perspective for solving large complex computing and it is a good way of optimisation.

In this work, we discuss the effectiveness of the threshold segmentation algorithm. Therefore, semantic segmentation of images is a very important task in computer vision. If you can quickly and accurately do image segmentation, many problems will be solved. In the future work, we will explore a semantic segmentation algorithm based on deep learning.

Acknowledgements

This work was supported by National Natural Science Foundation of China (No.61771416) and National Natural Science Foundation of China (No.61471311), CERNET Innovation Project (No.NGII20160510) and the Funds for Creative Research Groups of Higher Education of Xinjiang Uygur Autonomous Region (No.XJEDU2017T002). The authors would like to thank the anonymous reviewers for their constructive comments that helped to improve the quality of this paper.

References

Cheng, S., Lai, H., Wang, L. et al. (2018) *Vis Comput.* [online] https://doi.org/10.1007/s00371-018-1583-x.

Fan, J.L., Zhao, F. and Zhang, X.F. (2007) 'Recursive algorithm for three-dimensional Otsu's thresholding segmentation method', *Acta Electronica Sinica*, Vol. 35, No. 7, pp.1398–1402.

Felzenszwalb, P.F. and Huttenlocher, D.P. (2004) 'Efficient graph-based image segmentation', *International Journal of Computer Vision*, Vol. 59, No. 2, pp.167–181.

Garcia-Lamont, F., Cervantes, J., López, A. et al. (2018) 'Segmentation of images by color features: a survey', *Neurocomputing*, Vol. 292, pp.1–27.

Jiang, F., Qing, G.U., Hao, H.Z. et al. (2017) 'Survey on content-based image segmentation methods', *Journal of Software*, Vol. 28, No. 1, pp.160–183.

Jing, X.J., Ni, C.A. and Ao, S.J. (2001) 'Image segmentation based on 2D maximum between-cluster variance', *Journal of China Institute of Communications*, Vol. 22, No. 4, pp.71–76.

Lei, W., Duan, H. and Wang, J. (2008) 'A fast algorithm for three-dimensional Otsu's thresholding method', *IEEE International Symposium on It in Medicine and Education*, IEEE, pp.136–140.

Lin, N.I., Gong, Q., Cao, L. et al. (2013) 'Two-dimensional Otsu image segmentation algorithm based on adaptive weighted median filter', *Application Research of Computers*, Vol. 22, No. 2, pp.598–600.

Liu, J. (1993) 'The automatic thresholding of gray-level pictures via two-dimensional Otsu method', *Acta Automatica Sinica*, Vol. 19, No. 1, pp.101–105.

Liu, J., Tang, Q.H., Yu, Z.B. et al. (2014) 'Fast minimum error thresholding based on dimension reduction and rebuilding of the 3-dimensional histogram', *Journal of Electronics and Information Technology*, Vol. 36, No. 8, pp.1859–1865.

Liu, X., Yang, L. and Polytechnic, L. (2018) 'Active contour image segmentation model based on weighted global image fitting energy', *Journal of Electronic Measurement and Instrumentation*.

Nickfarjam, A.M., Soltaninejad, S. and Tajeripour, F. (2014) 'A novel supervised bi-level thresholding technique based on particle swarm optimization', *Arabian Journal for Science and Engineering*, Vol. 39, No. 2, pp.753–766.

Otsu, N. (1979) 'A threshold selection method from gray-level histogram', *IEEE Trans Smc.*, Vol. 9, No. 1, pp.62–66.

Qing, X.U. and Fan, J.L. (2017) 'New three-dimensional Otsu segmentation algorithm based on decomposition histogram', *Transducer and Microsystem Technologies*, Vol. 36, No. 1, pp.119–126.

Shen, X.J., Long, J.W., Chen, H.P. et al. (2011) 'Otsu thresholding algorithm based on rebuilding and dimension reduction of the 3-dimensional histogram', *Acta Electronica Sinica*, Vol. 39, No. 5, pp.1108–1114.

Wang, Q., Zhao, H., Wu, W. et al. (2012) 'Algorithm for segmentation based on an improved three-dimensional Otsu's thresholding', *International Conference on Computer Science and Network Technology*, IEEE, pp.1737–1740.

Wen, H. and Wang, L. (2017) *Cluster Comput*. [online] https://doi.org/10.1007/s10586-017-1389-z.

Xiao, J., Jian, L.I. and Yu, L. (2003) 'Image segmentation based on 3D maximum between-cluster variance', *Acta Electronica Sinica*, Vol. 31, No. 9, pp.1281–1285.

Zhang, J., Zuo, J., Zhong, T. et al. (2016) 'A new bone tissue segmentation algorithm based on the decomposition of three-dimensional Otsu', *Chinese Journal of Medical Imaging*, Vol. 24, No. 3, pp.218–222.

Zhiwei, Y.E., Wei, X.U., Zhao, W. et al. (2016) 'A 3D Otsu thresholding method based on improved firefly algorithm', *Chinese Journal of Stereology and Image Analysis*, Vol. 21, No. 4, pp.374–380.